The International Journal of Advanced Manufacturing Technology (2026) 145:2159–2179
https://doi.org/10.1007/s00170-026-18414-w

ORIGINAL ARTICLE

Potential primary energy and cost savings through industrial symbiosis: Aluminum chips-to-feedstock strategies for additive manufacturing

Maria Gloria Trapani[1] · Simone Amantia[1] · Livan Fratini[1] · Giuseppe Ingarao[1]

Received: 12 March 2026 / Accepted: 26 May 2026 / Published online: 12 June 2026

Abstract
With global aluminum demand on the rise and the sector's high energy intensity, the development of energy and resource-efficient manufacturing strategies has become increasingly important. During aluminum production, a large portion of material is lost before reaching the final product, making near-100% material reuse a key objective. Conventional recycling methods, based on remelting, offer advantages over primary production in terms of energy savings; however, they still present significant limitations, particularly when dealing with machining waste such as chips, which are prone to oxidation and quality degradation. In this context, industrial symbiosis emerges as a promising approach, to reduce waste generation by promoting circular material flows within and across manufacturing systems. However, implementing such strategies poses several challenges, including the need to manage material quality and compatibility. This study presents a comprehensive environmental and economic model of the entire process chain, from material process scrap recovery to final component production. The analyses are applied to compare four manufacturing routes: subtractive manufacturing, WAAM-based production, and two industrial symbiosis configurations integrating a solid-state recycling process, namely Friction Stir Extrusion, to generate WAAM-based feedstock. The analysis demonstrates that symbiotic strategies can significantly reduce energy use, material consumption and resource depletion. However, further process optimization is required to fully unlock their cost-effectiveness and industrial scalability.

Keywords Industrial Symbiosis · Energy demand · Cost · Solid-state recycling · Additive manufacturing · LCA

1 Introduction

In recent years, global aluminum demand has continued to increase, with a steady growth in production volumes largely driven by industrial development in Asia [1]. Due to the energy-intensive nature of the aluminum industry worldwide, this trend has a significant impact on the environment. Currently, the sector generates an estimated 270 million tons of CO_2 emissions annually, accounting for nearly 3% of global direct CO_2 output [2]. About 62% of these emissions are associated with the energy required for production processes. Furthermore, material efficiency remains a critical issue: data from 2024 reveal that approximately 15% of the aluminum produced becomes manufacturing scrap (also called "new scrap") before reaching the final product stage [3]. This material is recyclable; however, as highlighted by Atherton [4], although recycling is the most effective strategy for managing metals, offering both economic and environmental benefits, its conventional implementation relies predominantly on remelting. While remelting is considerably more energy-efficient than primary production, it still presents a major challenge due to the high oxygen affinity. This challenge is particularly critical in the case of machining waste, such as aluminum chips (also called turning scrap), which, due to their morphology are characterized by a high surface-to-volume ratio [5]. During the production of this type of manufacturing waste, the fraction of the material that wasn't exposed to the atmosphere comes into contact with the oxygen in the environment and forms the Al2O3 as a thin oxide layer on the chip

✉ Giuseppe Ingarao
giuseppe.ingarao@unipa.it

[1] Department of Engineering, University of Palermo, Viale delle Scienze, Palermo 90128, Italy

surface. This fraction of material cannot be recycled and represents an initial share of permanent material loss. Once the chips are introduced into the aluminum melt, their low bulk density causes them to float on the melt, resulting in a permanent loss close to 16% when flux treatment is applied [6] or even higher losses ranging from 20 to 25% with alternative remelting strategies [7]. To address this limitation, SSR techniques have emerged as a viable alternative: since these processes consolidate aluminum chips below the melting point, the formation of Al2O3 and the related material losses are inherently avoided [8, 9]. Evolving from the Friction Stir Welding (FSW) process, SSR enables the recovery of metallic materials without the need for remelting. These methods are fundamentally based on the solid bonding phenomenon, which requires (*i*) the application of high pressure, (*ii*) elevated temperatures, often generated by frictional heat between process components, and (*iii*) sufficient processing time to allow proper material consolidation [10].

Therefore, considering the current production scenarios and the growing environmental concerns associated with manufacturing processes and recycling strategies, there is a pressing need to reimagine industrial streams from new perspectives [11]. Industrial symbiosis, first proposed by Frosch and Gallopoulos in 1989 [12], drawing inspiration from natural ecosystems, emerges as a promising strategy. What is waste for a process becomes a resource for another. Through this circular lens, over the years, several processes (including SSR) have been identified as potential "sink" for waste to create symbiotic links between different production systems, enabling near 100% reuse of materials [13]. However, industrial symbiosis implementation continues to face several important challenges. First, despite its recognized potential, the number of systematically investigated symbiotic process chains remains limited, and many possible source–sink combinations are still unexplored. Then, the lack of standardized methodologies, particularly in Life Cycle Assessment (LCA), makes it difficult to consistently quantify environmental benefits and compare alternative solutions, as the symbiotic processes implies the multi-functionality problem, since the waste is reclassified as by-product. In addition, significant technological barriers persist, especially those related to the variability, contamination, and quality of manufacturing scrap, which often require additional pre-processing steps (e.g., cleaning, re-alloying), potentially increasing both environmental and economic burdens. In this regard, the cost-effectiveness of symbiotic strategies, along with their energy-efficiency, remain critical factors for industrial adoption. These limitations highlight that, although industrial symbiosis represents a promising pathway toward more sustainable manufacturing, further research is needed to systematically identify viable symbiotic links and to overcome both methodological and technological gaps. Recent research has shown that a closed-loop industrial symbiosis approach can be implemented by integrating friction stir extrusion (FSE) with friction-based additive manufacturing [14]. This strategy facilitates the immediate recycling of production waste, such as AA6082 heat-treatable aluminum alloy chips, within the same factory setting, through a two-step process that promotes a more sustainable and resource-efficient production cycle. Moreover, it has been confirmed that aluminum rods produced via FSE from recycled chips are suitable for single-bead additive deposition; however, multilayer builds remain constrained by severe porosity (density ≈ 77%), indicating that stricter control of hydrogen-related effects and further process optimization are still required [15]. The observed porosity trends further indicate that defect concentration increases in regions that solidify at later stages of the deposition process, a behavior that can be attributed to the high solubility of hydrogen in liquid aluminum. Optimization of wire deposition process parameters remains an area of investigation, showing promising potential. From the economic perspective, preliminary evaluations, such as those involving the use of chip-compacted bars as AFSD feedstock [16], have begun to address this issue, though comprehensive assessments are still limited in literature. Furthermore, machining waste is frequently poorly managed, with aluminum chips from different alloys commonly collected in a single container. These mixed scraps are typically sent to recycling facilities, where the material undergoes what is often commonly referred to in literature as open-loop recycling. Such an approach inevitably leads to a loss of the original alloy quality, known as downcycling [17]. Strategies like dilution can be employed to restore the desired alloy composition. An alternative pathway is the closed-loop approach, which involves remelting chips originating from a single alloy type, thereby preserving the chemical balance and enabling the recovery of the original alloy composition after remelting [18].

This work aims to assess both the environmental and economic impact of industrial symbiosis strategies compared to traditional manufacturing methods. Although the aforementioned studies including SSR techniques, a clear gap exists regarding the development of a unified modelling approach capable of capturing the full process chain, from material recovery to final component production, while simultaneously accounting for material losses, energy consumption, environmental impact, and production costs. Most of the existing studies are limited either to specific process stages or to the production of semi-finished products, without extending the analysis to the complete manufacturing pathway and the final component. A first environmental impact assessment of the FSE process was presented in [19], focusing on the production of a rod; however, the symbiotic link was not considered. In that study, indeed, a 5 mm diameter rod was produced, and no subsequent processing steps were included in the analysis. Similarly, previous research on the environmental impact of chips recycling through SSR has typically been limited to the production of semi-finished products [20], such as billets or wires. Although some technological demonstrations of symbiotic approaches have been reported in literature [15], these studies do not provide a comprehensive modelling of the entire manufacturing pathway from both environmental and economic perspectives. In this context, the present study aims to develop and apply a comprehensive model of the full process chain for the proposed symbiotic strategies, focusing on the AA6082 alloy. The objective is to quantitatively assess the environmental and economic performance of the proposed strategy through the combined evaluation of environmental impacts and production costs, and to compare these results with those of conventional manufacturing routes. Differently from previous studies, the proposed approach adopts a cradle-to-gate perspective and extends the assessment from the recycling stage to the final component production, enabling a more comprehensive evaluation of the environmental and economic implications of the symbiotic manufacturing pathway.

Specifically, the assessment focuses on two distinct symbiotic pathways for producing feedstock for the Wire Arc Additive Manufacturing (WAAM) process compared with a pure subtractive approach and a WAAM process performed with conventionally manufactured wire. The two symbiotic configurations differ based on the origin of the recycled material: one uses externally sourced aluminum chips, while the other relies on chips generated in-situ (therefore internally) during the machining process. It is important to emphasize that the novel internal approach proposed in this work aims to monitor and control internal scrap flows, avoiding the mixing of waste from different aluminum series. This is a key factor in preventing the aforementioned downcycling phenomenon, thereby preserving the quality of recycled material and promoting a more effective, high-value circular economy. In a real industrial context, re-alloying could be necessary if the alloy information is lacking. However, in the symbiotic approaches considered here, re-alloying is not required, as all input alloys are assumed to be fully traceable. Ensuring transparency of symbiotic flows is one of the main challenges of industrial symbiosis implementation. The analysis is initially performed on two fixed geometry shapes, then it is decided to extend the analysis to a wide range of shape complexities, with a focus on the Solid-to-Cavity Ratio (SCR) measure. This choice is motivated by the well-established relevance of SCR when comparing additive and conventional manufacturing processes. Generally, lower SCR values imply high energy efficient performance in AM processes due to reduced material usage [21, 22].

The findings of this study provide insights into the potential benefits and trade-offs of industrial symbiosis implementation in the manufacturing environment. Indeed, the introduction of symbiotic practices yields environmental benefits on three levels: a significant reduction in energy consumption throughout the production cycle, a decrease in the use of raw materials, and a reduction in chip generation, whether from internal processes or third-party industries. This approach promotes a more resource-efficient manufacturing process aligned with global sustainability goals. From an economic standpoint, however, further improvements in the process setup are still required for symbiotic approaches to become the most convenient option, even when considering only production costs.

2 Methodology

A comparative analysis is conducted to evaluate the sustainability performance of the manufacturing processes examined in this study (see paragraph 2.3). Both the environmental and economic dimensions are deepened, using Cumulative Energy Demand (CED) and total production cost as key metrics. Specifically, CED was chosen due to its widespread use, ease of implementation, and straightforward interpretability. Then, to further investigate the environmental performance of the proposed manufacturing routes, an LCA under a different metric was conducted in accordance with ISO 14,040/44 standards, and the results are presented in Sect. 5.

2.1 System boundaries for environmental assessment

A life cycle approach is adopted to assess the environmental impact, with a cradle-to-gate plus End of Life (EoL) system boundary. The impact of raw material production, premanufacturing, manufacturing (including post-processing when needed) and recycling have been evaluated. Recycling benefits are included into the embodied energy of material production according to the well-established recycled content method proposed by Hammond and Jones [23]. In accordance with this method, the benefits associated with recycling are allocated to the upstream stage of the product system, thereby reducing the embodied energy relative to that of virgin materials, as the input material contains a recycled fraction. The use of recycled material is thus considered beneficial due to the lower impact of its production. Use phase was neglected as it is assumed to be the same for the different manufacturing scenarios focus of this study.

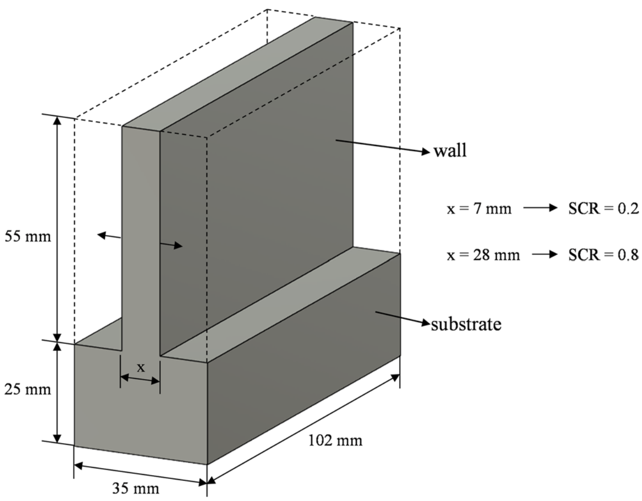

Fig. 1 Analyzed case study

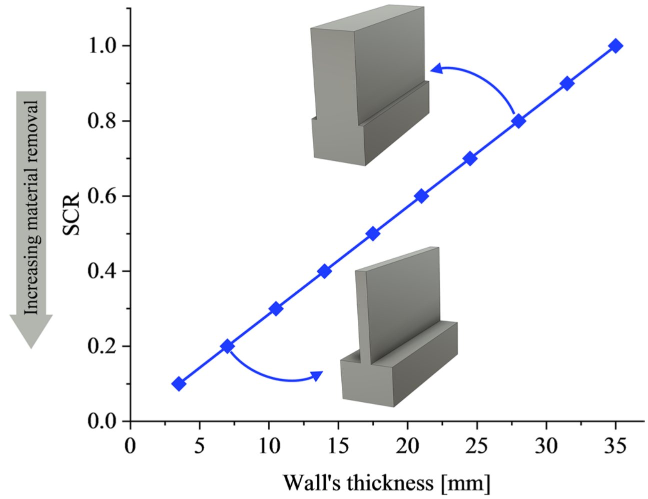

Fig. 2 Solid-to-cavity ratio as a function of the geometry shape

This is justified by the nature of DED processes, which, differently from powder bed technologies, typically do not allow for topology optimization. The limited potential for lightweight structural design cuts back any significant environmental benefits during the use phase, such as reduced fuel consumption in transportation applications [24]. Consequently, in the absence of weight reductions enabled by design optimization, the impact during use phase is considered negligible and is excluded from the comparative evaluation. The selected methodological approach allows for a detailed allocation of environmental burdens within each life cycle stage within the defined system boundaries and facilitates the comparison of the alternative manufacturing routes.

2.2 Case study presentation

The functional unit used for environmental and economic assessment consists of a T-shaped cross-sectional component. The material used is a 6xxx series aluminum alloy, as the aim of this study is to explore the environmental and economic feasibility of industrial symbiosis strategies. This alloy facilitates the establishment of symbiotic links, as both experimental and literature data are available for the selected manufacturing processes. Its geometry and dimensions are provided in Fig. 1. It comprises two main elements: a substrate and a vertical wall. This distinction is important as, based on the manufacturing route selected, the substrate will be treated as conventionally manufactured while only the vertical wall will be additively deposited, an arrangement that reflects the hybrid nature of the considered process. The substrate dimensions remain constant, while the wall thickness varies depending on the scenario. The analysis is indeed initially performed considering two distinct wall thicknesses, 7 and 28 mm, representing two geometry complexity levels, which can be described by the Solid-to-Cavity Ratio (SCR) measure. As defined by Morrow et al. [22], the SCR is the ratio of the final part volume to the volume of its bounding box (represented by the dashed line in Fig. 1). This factor is particularly significant in the context of subtractive manufacturing, where a low SCR implies a high amount of material removal, increased machining operations, and consequently greater part complexity. In Fig. 2, the correlation between the wall's thickness and the SCR value is shown, highlighting the two reference cases analyzed (SCR = 0.2 and SCR = 0.8). These geometric configurations define the functional units adopted for the LCA. Then, to further investigate the influence of geometry complexity on environmental and economic performance, the thickness value has been varied over a broader range. This allowed for the evaluation of energy and cost trends associated with varying SCRs.

2.3 Manufacturing approaches considered

In the present study, four manufacturing approaches are evaluated and they can be grouped into two main categories: conventional machining and additive-based processes. The latter category involves the deposition of the wall through a direct energy deposition (DED) technique, specifically WAAM, widely used with different structural alloys [25, 26]. Within this category, three scenarios are explored, two of which incorporate the principles of the industrial symbiosis.

This choice is motivated by the relevance of material efficiency and recycling in aluminum component manufacturing. The selected routes represent strategies that differ in material utilization, feedstock form, and process integration, while remaining comparable for discrete part manufacturing. Other manufacturing routes, such as casting and forging, were excluded as they are primarily suited for mass production and strongly influenced by batch size, limiting their comparability in this context. Similarly, alternative additive processes were not considered due to differences in material feedstock and limited data availability.

The manufacturing pathways analyzed are summarized below, with the corresponding process flows illustrated in Fig. 3:

(a) *Machining approach*: the desired T-shaped part is produced entirely through milling operations starting from an input workpiece, corresponding to the entire bounding volume of the final component. This process inherently results in high material waste, particularly as the wall thickness decreases. Most of the material is removed during a roughing stage, while the final 1 mm allowance on each surface is machined off by means of finishing operations.

(b) *WAAM-based approach*: the substrate of the component is fabricated via conventional methods, while the vertical wall is deposited using WAAM. The feedstock employed is commercially available aluminum wire, which is typically manufactured through conventional processes such as hot extrusion followed by wire drawing.

(c) *External symbiotic approach*: in this case the wire feedstock for WAAM process is produced starting from aluminum chips generated originating from external industrial machining operations, outside the system boundaries of the current analysis. These external chips are then consolidated into wire using the Friction Stir Extrusion (FSE) process, which serves as the symbiotic

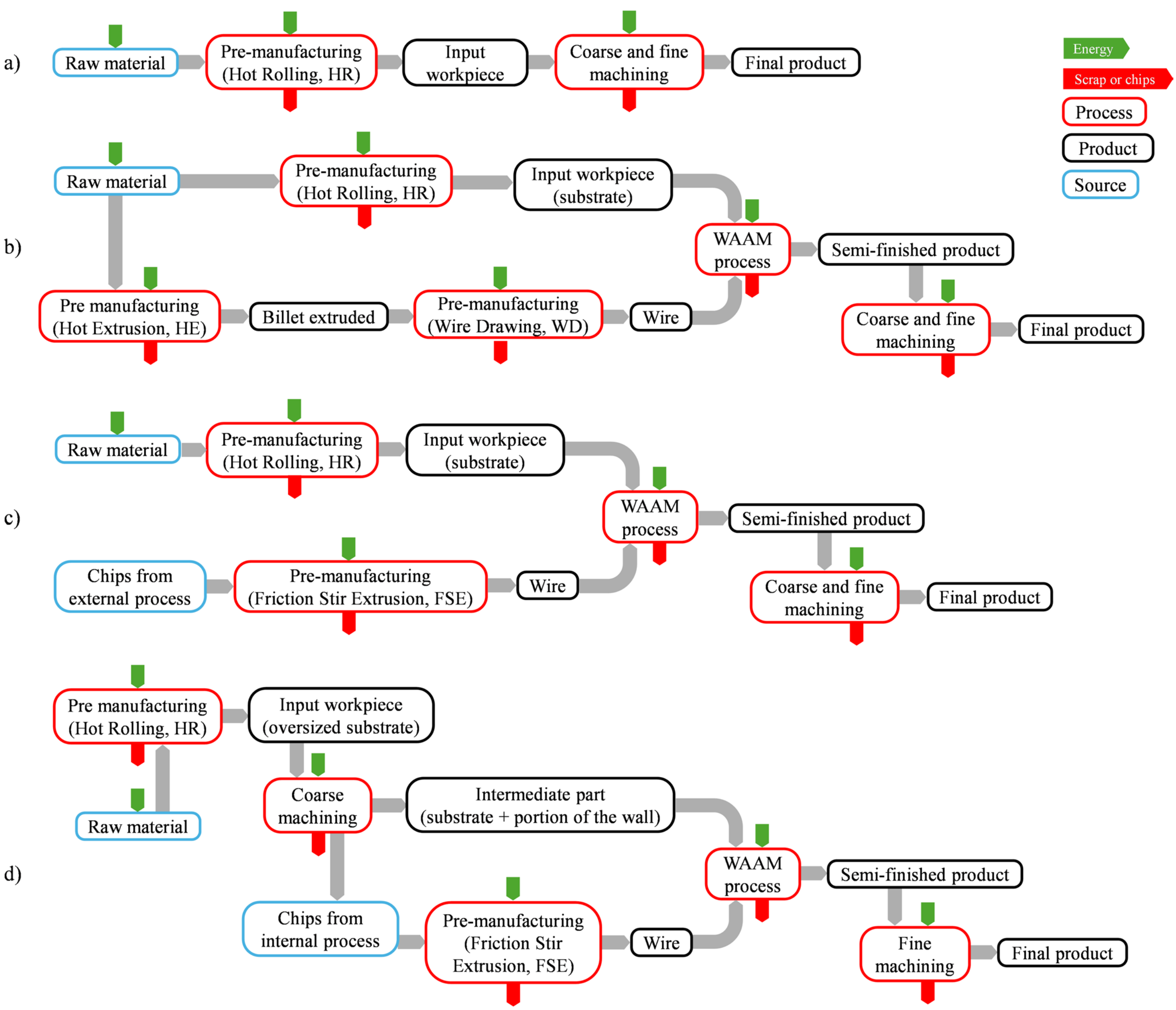

Fig. 3 Cradle-to-gate system boundaries for the (**a**) machining, (**b**) WAAM-based, (**c**) external symbiotic and (**d**) internal symbiotic approaches

link to convert waste material into usable WAAM feedstock.

(d) *Internal symbiotic approach*: here the aluminum chips used for wire production are produced internally during the machining of the substrate component itself. The substrate is oversized in height, allowing for (*i*) machine a portion of the vertical wall and (*ii*) generate aluminum chips for wire production, in order to deposit the remaining wall's height. Also in this case, the closed-loop material utilization is facilitated by the FSE process. A schematic representation of this approach is provided in Fig. 4. This approach helps to get over the uncertainties associated with the quality and composition of chips sourced from third-party suppliers. By managing chip flows internally, it is possible to ensure the use of a single, well-defined aluminum alloy, thereby avoiding the risk of cross-contamination with other alloy types.

In the context of approaches b, c, and d, the semi-finished product corresponds to the component (the wall deposited onto the substrate), which requires subsequent finishing operations to reach its final form. In turn, when considering the approach a), coarse and fine machining operations are considered as a single step; therefore, in the corresponding process flow diagram, the input workpiece becomes directly the final product. It should be noted that Fig. 3 illustrates the mass and energy flows qualitatively; the corresponding quantitative values are discussed in Sect. 3.1.

The concept of industrial symbiosis in this study lays in the conversion of the aluminum chips, machining waste, as valuable input, thus resource, for another process. As mentioned, the selected intermediate process enabling the symbiotic link is the FSE, which transforms aluminum chips into wire feedstock for the sink process (WAAM deposition) with satisfactory mechanical properties and high material efficiency [19]. During FSE, once the chips are compacted

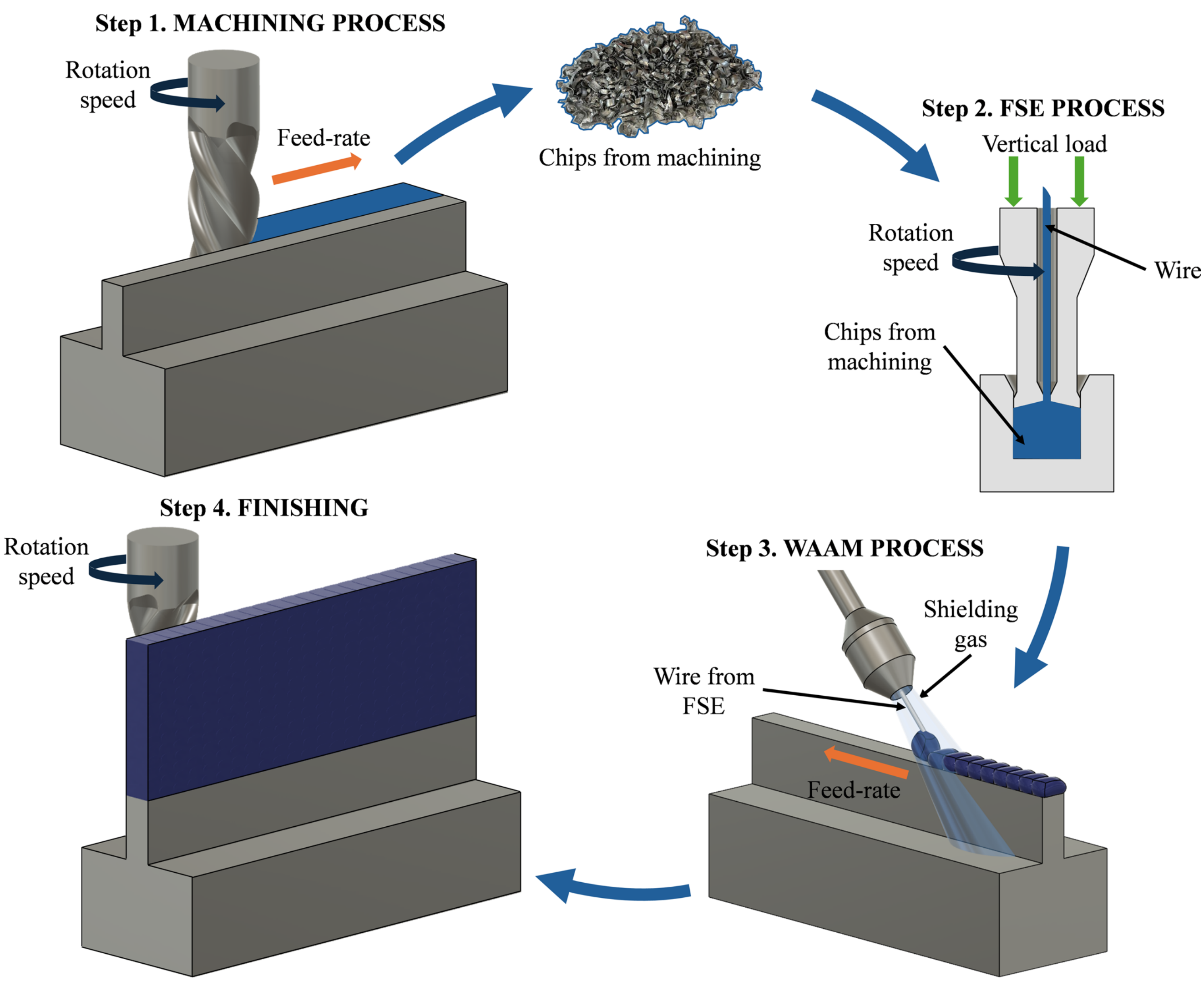

Fig. 4 Schematic representation of the Internal symbiotic approach

within a closed die, the rotation of a tool featuring a Ø1.2 mm hole at the interface with the material, combined with the application of a vertical load, creates the conditions necessary to trigger solid bonding. The combined effect of heat, pressure, and strain rate, after the required processing time, leads to the fracture of the thin aluminum oxide layers that naturally form when aluminum and its alloys come into contact with oxygen. These specific process conditions promote oxide fragmentation, enabling intimate metal-metal contact between chips. During the bonding phase, aluminum oxide residues remain entrapped within the wire produced by the extrusion process, making it impossible to completely eliminate them. Moreover, it requires less energy than conventional recycling routes involving the remelting process [27]. Previous investigations conducted by one of the authors have highlighted that, in aluminum alloys, the combined influence of frictional heating and severe plastic deformation during FSE not only assists in breaking up the oxide layer but also induces substantial microstructural transformations within the extruded material. These results showed that, under appropriately selected processing conditions, the extruded wire can undergo full recrystallization and develop a fine and equiaxed grain structure throughout the section. Such refinement arises from the interplay between high deformation levels and localized thermal input, which can bring the alloy to a condition comparable to the T3 temper, although the absence of post-extrusion cold working limits further precipitation strengthening.

For clarity, both the external and internal symbiotic approaches are WAAM-based, as the wire produced through FSE is deposited using the same method as in the standard WAAM scenario (indicated as b). The alternative naming is adopted just for conciseness and to emphasize the different feedstock sourcing strategies. Although the four approaches may lead to components with different mechanical responses, it is assumed, consistent with common practice in literature [21], that each manufactured part satisfies the intended functional requirements and conforms to the geometric specifications defined in the original design.

2.4 Models used to quantify energy and costs

This section describes the models employed to assess energy consumption and production costs. The modeling frameworks used in this study have been adapted from established approaches presented in previous studies [21, 28].

The metric used to evaluate the environmental impact is CED. Concerning the costs, a model comprising production cost for a single part is considered. Therefore material, indirect, labour and processing costs are summed together.

Since there are no economies of scale involved in the processes analyzed in this work, only one part to be produced is considered as a functional unit. The evaluation of the selected metrics, both CED and costs, is based on the cumulative contributions of each phase defined within the system boundaries (as drawn in Sect. 2.1) for each manufacturing route analyzed in this work.

2.4.1 CED modeling framework

The CED associated with each manufacturing strategy is evaluated as the sum of contributions coming from each manufacturing stage, accounting therefore for the total energy required throughout the production stages within the defined system boundaries, ranging therefore from raw material production to manufacturing and post-processing. For clarity, the analysis is carried out at a primary energy level by using the conversion factor η, to include transmission losses occurring during the conversion from primary to delivered energy [29]. In each approach the material feedstock mass, which corresponds to the mass to be purchased in the next cost modeling, is calculated accounting for process inefficiencies (through input/output ratios) and scrap, as chips and allowances.

The total primary energy per part manufactured by conventional machining was computed as detailed in Eq. (1). A conventional milling process has been considered, in line with the geometric complexity of the required features.

$$E^{machining} = \overbrace{\left[\left(m_p + m_c^{rough} + m_c^{fin}\right)\cdot y_{HR}\right]\cdot\left(E_E + E_{HR}\right)}^{E_{material\ production+pre-manufacturing}} + \overbrace{\left[\left(m_c^{rough}\cdot SEC_{milling}^{rough}\right) + \left(m_c^{fin}\cdot SEC_{milling}^{fin}\right) + E_{idle}^{CM}\right]\cdot\frac{1}{\eta} + E_{cf}}^{E_{manufacturing}} \quad (1)$$

Where:

- m_p (kg): mass of the part to be produced;
- m_c (kg): mass of the chips differentiated by roughing and finishing operations;
- y_{HR}: input/output ratio of Hot Rolling process;
- E_E (MJ/kg): embodied energy for material production;
- E_{HR} (MJ/kg): energy demand for hot rolling;
- $SEC_{milling}$ (MJ/kg): Specific energy consumption of milling process differentiated by roughing and finishing operations;
- E_{idle}^{CM} (MJ): idle energy consumption during machining;
- E_{cf} (MJ): energy associated with cutting fluid.

It is important to note that both the E_{idle}^{CM} and $E_{cf.}$ factors depend on variables that are not constant. Specifically, idle energy consumption is computed as the product of the machine's stand-by power and idle time. The same approach will be applied to the idle energy consumption in WAAM processes. The energy associated with cutting fluid is calculated as the product of the fluid consumption rate (kg/h), the cutting time (h), and the embodied energy of the cutting fluid (MJ/kg).

The WAAM-based route (Eq. 2) includes energy contributions from wire production (i.e., hot rolling, hot extrusion and wire drawing), material deposition, and subsequent finishing. The material input is calculated by applying cumulative input/output ratios for each stage of the production chain.

$$E^{WAAM} = \overbrace{[(m_p + m_a) \cdot y_{HE} \cdot y_{WD} \cdot y_W] \cdot (E_E + E_{HE}) + [(m_p + m_a) \cdot y_{WD} \cdot y_W] \cdot E_{WD}}^{E_{material\,production+pre-manufacturing}} + \overbrace{\left\{[(m_p + m_a) \cdot y_W] \cdot SEC_{WAAM} + (m_a \cdot SEC^{fin}_{milling}) + E^{WAAM}_{idle}\right\} \cdot \frac{1}{\eta} + E_{gas}}^{E^{WAAM}_{manufacturing}} \quad (2)$$

Where:

- m_p, m_a (kg): mass of the part and of the allowance;
- y_w, y_{WD}, y_{HE}: input/output ratios of WAAM, wire drawing and hot extrusion processes;
- E_{WD} (MJ/kg): energy demand for wire drawing;
- SEC_{WAAM} (MJ/kg): Specific energy consumption of WAAM process;
- E^{WAAM}_{idle} (MJ): idle energy consumption during WAAM;
- E_{gas} (MJ): energy associated with gas consumption.

Similarly to the approach used for cutting fluid energy, the energy associated with gas consumption is calculated as the product of the gas consumption rate (q_{gas}), the deposition time and the CED of Argon gas.

For the external symbiotic approach, the CED of which is described in Eq. (3), the burden related to chips cleaning is included considering an alkaline bath. This energy accounts for the treatment of the chips' surface, and to this end the surface-to-mass ratio is included in the equation This is mainly because chips are always contaminated with lubricants and oils used during the machining process. Therefore, before being recycled through FSE they must be cleaned.

$$E^{ExtSymb} = \overbrace{[(m_p + m_a) \cdot y_W \cdot y_{FSE}] \cdot \left(SMR \cdot CED_{AlkBath} + SEC_{FSE} \cdot \frac{1}{\eta}\right)}^{E_{pre-manufacturing}} + E^{WAAM}_{manufacturing} \quad (3)$$

Where:

- y_{FSE}: input/output ratios of FSE process;
- SMR (m^2/kg): surface-to-mass ratio of metal chips;
- $CED_{AlkBath}$ (MJ/m^2): cumulative energy demand of degreasing process in the alkaline bath;
- SEC_{FSE} (MJ/kg): Specific energy consumption of FSE process.

For the internal symbiotic approach (Eq. 4) instead, the machining process needed to produce the chips for producing the wire for depositing the remaining wall, is considered in the pre-manufacturing step, along with the cleaning phase and the wire production through FSE. Since a comparative approach is carried out in this study, common elements can be disregarded as they are the same in each approach, this is the case of the substrate. Its production and premanufacturing are not considered in the formulations. Only for the internal symbiotic approach the additional height is considered through the m_x factor, which is precisely the mass of the exceeding part of the substrate.

$$E^{IntSymb} = m_x \cdot E_E + \overbrace{(m_c \cdot y_{FSE} \cdot y_W) \cdot \left(\frac{1}{\eta} \cdot SEC^{rough}_{milling} + SMR \cdot CED_{AlkBath} + \frac{1}{\eta} \cdot SEC_{FSE}\right)}^{E_{pre-manufacturing}} + E^{WAAM}_{manufacturing} \quad (4)$$

In these two last formulations (Eqs. 3 and 4), the energy associated with WAAM deposition is calculated as detailed in Eq. (3) and is indicated as $E^{WAAM}_{manufacturing}$, with the difference that in Eq. 4 the mass to be processed by WAAM is the mass of the chips (m_c) which of course considers also in this case the allowance to be machined off. It is worth remembering that in the internal symbiosis case, the mass of the part to be deposited is not the same as the other approaches (as part of the wall is reached via machining). The starting workpiece height was dimensioned with an intermediate height sufficient to generate, through partial machining, the aluminum chips required for producing the deposition wire, thereby enabling the completion of the part via additive deposition. Such a configuration enabled the creation of a closed-loop system with minimal material waste.

2.4.2 Cost modeling framework

The total cost for producing a single component, C_{part}, is computed by summing four main cost categories: material, indirect, labour and processing costs. This unified structure is applied consistently to all the manufacturing strategies under investigation.

Material cost is calculated as the product of the unit cost of the material feedstock and the total feedstock mass required to manufacture a single part. Indirect costs encompass equipment depreciation (based on a 10-year lifetime), maintenance, and administrative overheads. Indirect costs are determined using an annual machine utilization rate and are distributed over the entire duration for which the machine is engaged by the part, encompassing both active cutting/deposition time and non-productive phases such as setup and standby time. Labour cost is modeled as a function of machine time and operator employment intensity, with the latter adjusted via a coefficient γ. Processing cost includes energy-related expenses and consumables. The energy cost is derived from idle and operating energy consumption, using the unit cost of electricity. Consumables are process-specific and are treated accordingly. Finishing costs include the machining of allowance to reach the desired surface quality and are present in the additive-based routes.

To maintain clarity and avoid redundancy, the general cost formulation is presented in Eq. (5), with detailed definitions of each parameter provided below.

$$C_{part} = \overbrace{C_{mf} \cdot m_{mf}}^{Material} + \overbrace{C_{ind} \cdot (t_{idle} + t_{op})}^{Indirect} + \overbrace{C_{op} \cdot (t_{idle} + t_{op} \cdot \gamma)}^{Labour} + \overbrace{C_{EE} \cdot (E_{idle} + SEC \cdot m_p) + C_{consum} + C_{FM}}^{Processing} \tag{5}$$

Where:

- C_{mf} (€/kg): purchase cost of material feedstock (i.e., input workpiece for conventional machining, wire for WAAM, or chips for the external symbiotic path);
- m_{mf} (kg): mass of material feedstock required to produce the part. It is calculated considering process inefficiencies and allowances for finishing operations (as detailed in the CED formulations);
- C_{ind} (€/h): indirect hourly cost rate;
- t_{idle} (h): idle time, usually associated with machine setup and non-productive phases. For WAAM deposition also the inter-layer cooling time (dwell time), is accounted inside this term;
- t_{op} (h): effective operating time (cutting, deposition or extrusion depending on the process);
- γ : operator employment rate, ranging between 0 and 1 depending on process level automation;
- C_{EE} (€/kWh): cost of electrical energy;
- E_{idle} (MJ): electric energy consumption of the machine during idling;
- SEC (MJ/kg): Specific Energy Consumption of the process;
- m_p (kg): mass of the part to be processed;
- C_{consum} (€): cost of consumables;
- C_{FM} (€): cost of finishing operations.

This general formulation can be easily adapted to each manufacturing route. Indeed, to reflect the variability among different manufacturing strategies, each term can be process-specific and denoted with superscripts (e.g., SEC^{CM}, t_{idle}^{WAAM}, etc.).

As previously mentioned, the term C_{consum} varies significantly depending on the manufacturing process. In the conventional machining approach, it includes cutting tools, specifically, endmills with four cutting edges, as well as lubricants, according to Eq. (6).

$$C_{consum}^{CM} = \sum_{i=1}^{n} (C_{tool_i} \cdot \frac{t_{ci}}{T_i}) + C_{lub} \cdot q_l \cdot t_c \tag{6}$$

Where:

- C_{tool_i} (€/edge): cost of the cutting tool used in operation *i* (*i*=roughing or finishing);
- t_{ci} (h): cutting time for operation *i*;
- T_i: tool life for operation *i*;
- C_{lub} (€/kg): cost of lubricant;
- q_l (kg/h): lubricant consumption rate;
- t_c (h): total cutting time.

For WAAM deposition instead, shielding gas (typically Argon) is the major consumable used to prevent oxidation locally, and its consumption ranges from 20 l/min [30] to 14 l/min [31] when depositing aluminum. The cost associated is expressed as:

$$C_{consum}^{WAAM} = C_{gas} \cdot q_{gas} \cdot t_{dep} \tag{7}$$

With:

- C_{gas} (€/kg): unit cost of shielding gas;
- q_{gas} (kg/h): shielding gas consumption rate;
- t_{dep} (h): deposition time.

For clarity, since gas consumption is reported in l/min, the gas flow rate (q_{gas}) in kg/h was calculated assuming normalized conditions, with a gas density of 1.784 g/L.

In contrast, FSE does not require lubricants or shielding gas, thus the consumables cost is negligible. Finishing costs are estimated as machining cost applied on the allowance thickness to be removed through finishing operations.

3 Inventory data

To implement the energy and cost equations described in the previous section, collecting material-, process- and cost-related data is essential. The eco-properties of AA6082 were mainly sourced from Granta software, while process data came from both literature and experimental measurements (in the case of FSE). The dataset presented in this section was also employed to conduct the LCA analysis, with the inventory phase carried out in accordance with the ILCD guidelines [32].

3.1 CED inventory data

Input data used for CED modeling are summarized in Table 1. Regarding the subtractive process, to estimate the specific energy consumption (SEC) during milling, the empirical model proposed by Kara and Li [33], where $SEC = C_0 + C_1/MRR$, has been adopted. Since the coefficients C_0 and C_1 are machine-dependent, a generalized SEC value was obtained by averaging data from two industrial milling machines operating under real conditions: Fadal VMC4020 and MoriSeiki DuraVertical 5100. Material removal rate (MRR) values were chosen considering wet machining conditions, in order to enhance overall process efficiency. Based on this, the estimated SEC for roughing and finishing machining were 3.54 and 17.49 J/mm^3, respectively. The latter value (denoted as $SEC_{milling}^{fin}$ in the CED equations) was also applied to the WAAM-based and the two symbiotic approaches for finishing operations. Specifically, the machining approach route assumes a 1 mm finishing allowance, while the other manufacturing routes, based on WAAM deposition, assume 1.5 mm for the lateral surfaces and 3 mm for the top surface. These larger allowances are necessary due to the inherent surface roughness resulting from the layer-by-layer deposition of molten metal. The FSE input/output ratio was set equal to 1, reflecting steady-state operating conditions with negligible material loss, as confirmed by experimental studies on continuous wire production [34]. This assumption reflects the key difference with traditional remelting routes characterized by permanent material losses. Regarding WAAM deposition, an average SEC value was calculated based on the energy per unit length (J/mm) reported in [35], as well as an average deposition rate. To calculate the energy consumption of WAAM during idling (E_{idle}^{WAAM}), the power demand listed in the table was multiplied by the sum of the stand-by and dwell times (both defined in the next paragraph), resulting in a total of 1.39 MJ.

Table 1 Material- and process-related inventory data

Variable	Value	Source
Embodied energy, with recycling benefits, E_E (MJ/kg)	112	[36]
Recycled fraction in the current supply, R	0.47	[36]
Energy demand for Hot Rolling, E_{HR} (MJ/kg)	6.5	[36]
Energy demand for Hot Extrusion, E_{HE} (MJ/kg)	13.80	[36]
Energy demand for Wire Drawing, E_{WD} (MJ/kg)	53.90	[36]
Input/output material ratio for Hot Rolling, y_{HR}	1.05	[36]
Input/output material ratio for Hot Extrusion, y_{HE}	1.29	[36]
Input/output material ratio for Wire Drawing, y_{WD}	1.14	[36]
Input/output material ratio for WAAM, y_W	1.01	[37]
Input/output material ratio for FSE, y_{FSE}	1	[38]
Conversion factor of Italy, η	0.41	[39]
MRR^{rough} (cm^3/s)	1.89	[40]
MRR^{fin} (cm^3/s)	0.091	[40]
SEC_{WAAM} (MJ/kg)	2.8	[35]
SEC_{FSE} (MJ/kg)	66	*
Embodied energy of cutting fluid, $E_{cf.}$ (MJ/kg)	1.37	[41]
Consumption rate of cutting fluid, q_l (kg/h)	0.48	[42]
Energy consumption CM during idling, E_{idle}^{CM}(MJ)	0.66	[43]
Power demand WAAM during idling, P_{idle}^{WAAM} (kW)	0.8	[44]
Extrusion rate FSE (mm/s)	36	*
Deposition rate WAAM (kg/h)	0.9	[35]
Argon consumption (l/min)	13	[35]
Surface-to-mass ratio, SMR (m^2/kg)	1	[10]
$CED_{Alk\ Bath}$ (MJ/m^2)	0.20	[39]
CED_{Argon} (MJ/kg)	34.3	[39]

* Experimentally measured during FSE process

To ensure transparency and replicability, the experimental procedure adopted for the FSE process in this study follows the methodology described in [38], with some variations to the experimental setup. Specifically, the recorded value of SEC and extrusion rate were obtained using a rotational speed of 600 rpm and a tool force of 21 kN. The tool employed featured an external diameter of 14.7 mm and an extrusion channel of 1.2 mm. This setup matches the target wire diameter (1.2 mm) required for WAAM deposition. For the present study, the optimal configuration was selected based on the process parameters explored (i.e., vertical load and rotational speed) in order to achieve the lowest SEC value. This choice is justified by the fact that FSE remains a non-optimized process at a laboratory scale.

3.2 Cost inventory data

The unit cost of aluminum wire was established at 20 €/kg, based on real procurement data. In contrast, commercially available aluminum cuttings used in the external symbiotic approach were priced at approximately 1.25 €/kg [45]. It is worth mentioning that mixed-alloy chips are available at a lower cost (around 0.60 €/kg), but their use may lead to variations in mechanical properties or require additional processing steps, such as material separation or re-alloying, which would increase system complexity and overall processing time. The input workpiece, which has been processed by hot rolling, is priced at 15 €/kg, based on market data.

To estimate the indirect costs, capital investment in key equipment was considered. The acquisition costs for the WAAM and FSE systems were set at 180,000 € and 200,000 €, respectively. Machining-related indirect costs were considered by including a 200,000 € CNC milling machine. Annual maintenance expenses were estimated at 6% of the initial equipment cost [46], while a general overhead rate of 5.46 €/h was applied [31]. Machine costs were depreciated over a 10-year lifespan, considering an annual utilization rate of 57% [46]. This adjustment provides a more realistic estimate of hourly depreciation, reflecting typical machine usage in industrial settings. Electricity costs were evaluated using an average industrial price of 0.1899 €/kWh [47], as reported by Eurostat for non-household consumers in Europe.

Process idle times included 0.25 h for setup activities [44] and 0.24 h for interlayer cooling during WAAM deposition, based on a dwell time of 30 s/layer, consistent with typical ranges adopted for aluminum [35, 48, 49], with a single-layer thickness of 1.9 mm. Operating times were estimated by simply dividing the mass of material to be processed by the corresponding process rates (material removal, extrusion, and deposition rate, as reported in Table 1). Operating times were derived from the material removal rate, extrusion and deposition rates reported in Table 1, by simply dividing masses to be processed by these parameters. Argon cost was set at 1.15 €/kg [50], while lubricants and cutting tools used during machining cost 0.93 €/kg and 1.5 €/edge [21], respectively. Labour costs were evaluated considering an operator average hourly rate of 21.66 €/h [40], with an employment factor $\gamma = 0.33$ for WAAM deposition and FSE, while for machining process $\gamma = 1$.

4 Results and discussion

The collected inventory data were applied to the equations corresponding to each manufacturing route, and the resulting CED and cost outcomes for the selected SCRs are summarized and discussed in the following. To better understand and examine which individual factor of influences has the largest impact on energy consumption and costs, detailed breakdown analyses are presented in Figs. 4 and 5. Specifically, cost categories and energies requirements associated with each stage of manufacturing processes can be identified.

Looking at the CED results (Fig. 5), machining exhibits similar CED values for both SCR scenarios. This is attributed to the fact that the environmental impact of subtractive processes is largely driven by the embodied energy of the material involved, rather than processing energy. The external symbiotic route performs better than the WAAM-based route in terms of CED, as no impact related to material production is considered when chips are the input material. The chips environmental impact is mostly attributed to the FSE process, which is treated as a pre-manufacturing operation along with cleaning. The internal symbiotic route, however, shows a more complex behavior. At SCR = 0.2, it shows a higher energy demand than the external approach. This is primarily due to the significant contribution of the FSE process, characterized by a high SEC value (specifically, 66 MJ/kg). In this scenario indeed, the starting workpiece (properly dimensioned), has a low height, requiring a larger portion of the wall to be deposited via WAAM, and consequently, a greater volume of chips to be processed through FSE. As the SCR increases to 0.8, the CED of the internal symbiotic scenario becomes more favorable. With a higher starting workpiece height, both milling and deposition volumes are reduced. Only a small portion of the wall needs to be machined off and subsequently deposited. Therefore, this reduced shape complexity lowers the energy demand, especially on WAAM, and improves the overall energy performance of this manufacturing route.

From the economic perspective, depicted in Fig. 6, the machining approach is the most cost-efficient, regardless of the selected SCR scenario. This is mainly due to the streamlined process chain, involving only a single production step. As a consequence, indirect, labour and processing costs are limited to milling operations. Differently, the other three approaches involve multiple production steps. For instance, in the WAAM-based route, the finishing costs encompass all the cost items associated with milling, while in symbiotic approaches the indirect, labour, and processing costs additionally account for those related to the FSE process. When SCR = 0.2, the cost-efficiency ranking, from most to least convenient, is the following: Machining, WAAM-based, internal symbiosis and external symbiosis. At SCR = 0.8, the order shifts to: Machining, Internal Symbiosis, WAAM-based and External Symbiosis. This shift reflects how removal volumes and material deposition, as well as their associated processing times, directly affect the overall cost structure. The WAAM-based approach is sensitive to wire feedstock costs. As SCR increases from 0.2 to 0.8, the required deposition volume increases, leading to a higher proportion of total costs attributed to wire purchase. In contrast, symbiotic approaches benefit from lower material costs due to the reuse of material streams: in the external symbiotic case, feedstock is derived from low-cost aluminum chips; in the internal case only the additional substrate height is purchased (it is worth remembering that the common substrate is not considered in this comparative assessment). Despite the material cost advantage, the external symbiotic route consistently results in the highest overall cost. This is largely due to the inefficiency of the FSE process, which exhibits a low extrusion rate. This results in extended processing times and consequently higher indirect and labour costs. In the Internal symbiotic approach, production costs are distributed among three production steps (milling, FSE and WAAM). At SCR = 0.2, the high deposition and milling requirements result in greater processing time for the FSE and WAAM processes, increasing overall indirect and labour costs. However, at SCR = 0.8, both deposition and milling volumes are lower, which reduces

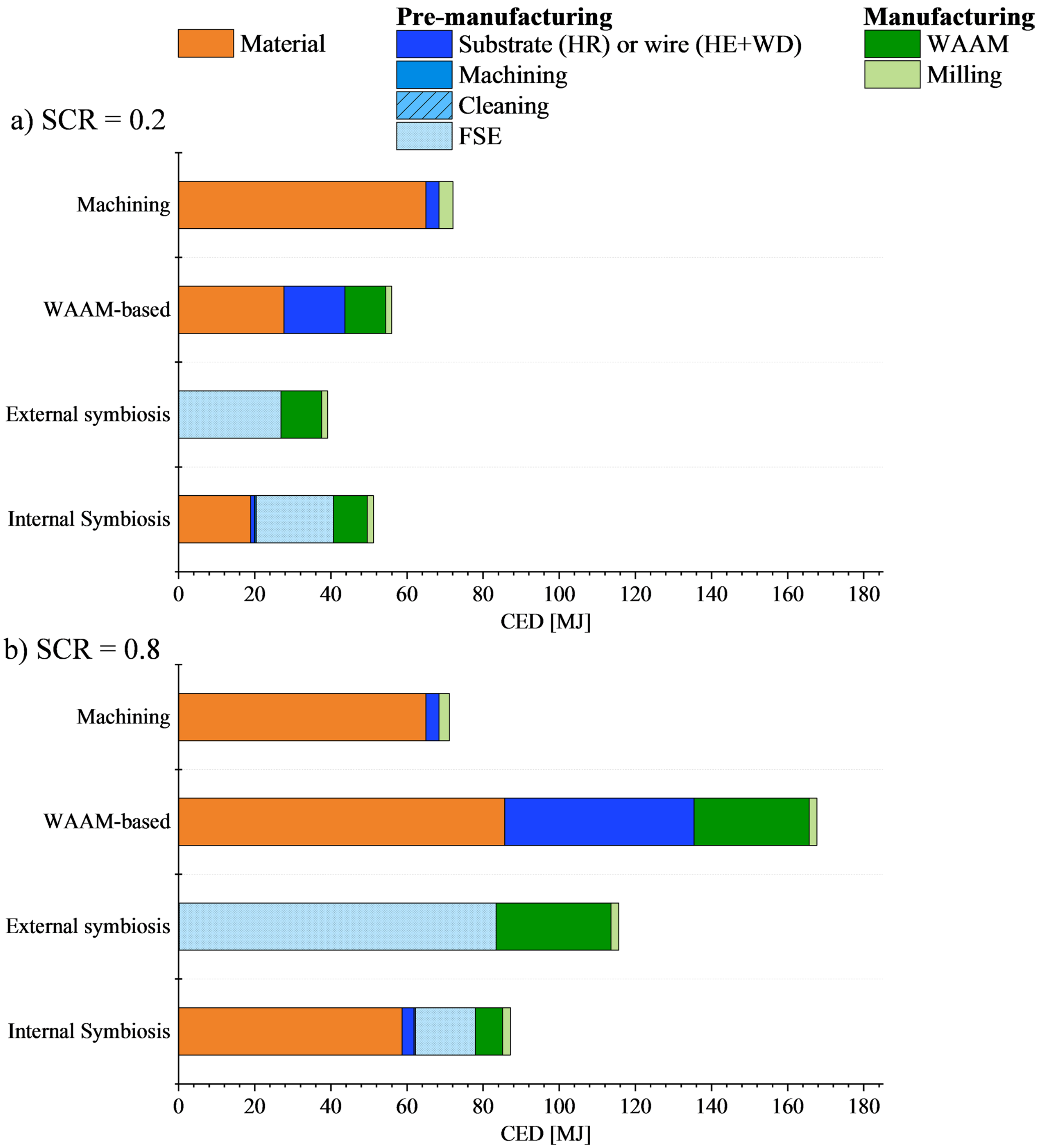

Fig. 5 Cradle-to-gate energy consumption results for (**a**) SCR = 0.2 and (**b**) SCR = 0.8

processing time and thus brings this route to a lower cost than WAAM-based.

A notable observation in all strategies is that indirect and labour-related costs dominate the overall cost structure, often exceeding raw material expenses. These categories are highly dependent on processing time and are therefore amplified in low-productivity systems, such as the laboratory-scale FSE unit used in this study. Improving the efficiency and scalability of these critical processes could substantially reduce costs. This, in turn, could make also external symbiotic strategies economically viable, even under different SCR conditions.

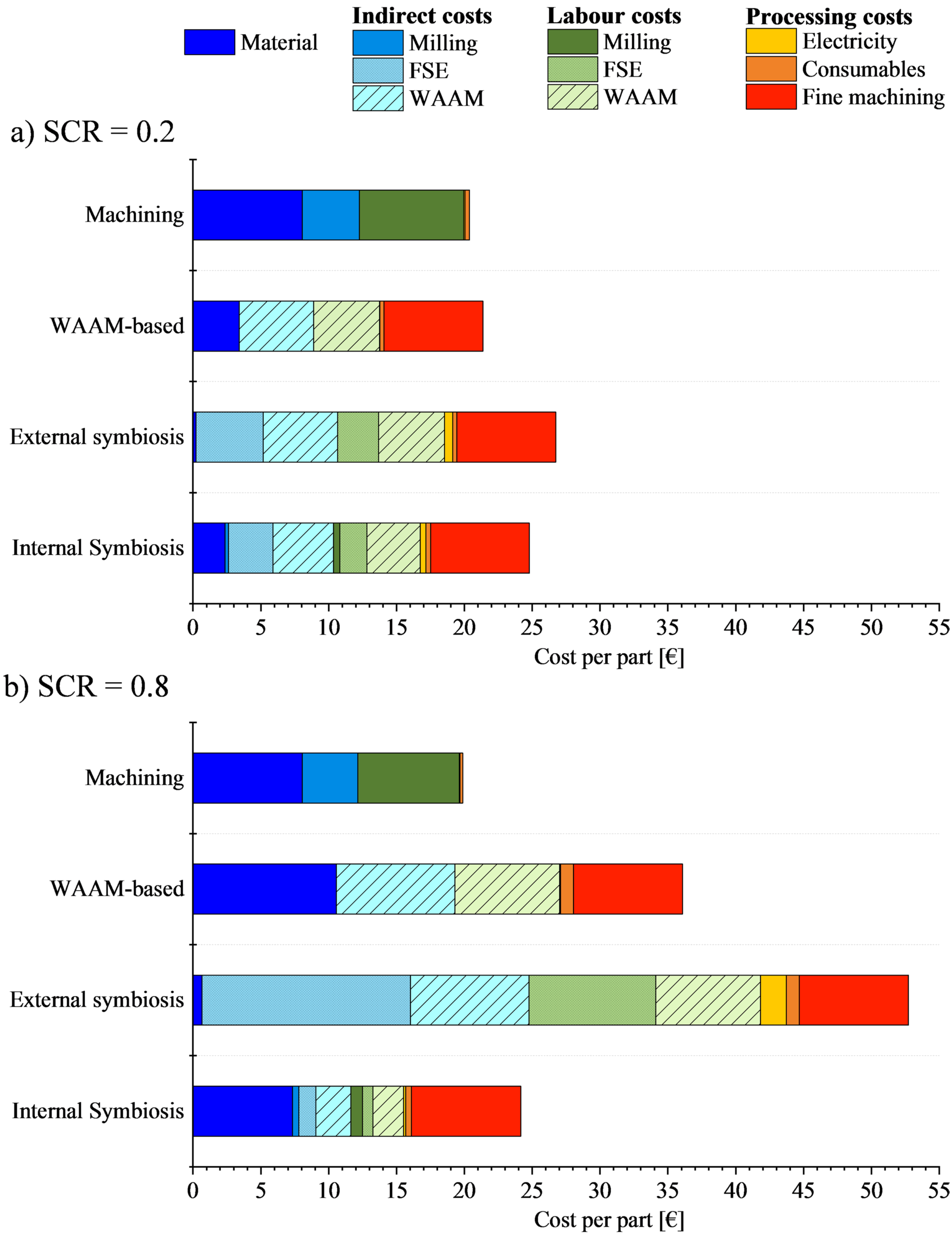

Fig. 6 Cost per part results for (**a**) SCR = 0.2 and (**b**) SCR = 0.8

4.1 Extension of the analysis with varying SCR

After having analyzed the fixed SCR case studies, the decision to extend the analysis to a continuous range of SCRs was made. To this aim the wall's thickness has been varied from 2.5 to 35 mm, allowing to analyze a wide range of geometry complexities (with SCR ranging from 0.071 to 1). In Fig. 7 it is possible to see energy and cost trends with varying SCRs.

In both CED and Costs graphs, Break-Even Points (BEPs) are observed where at least two curves intersect. These points represent threshold SCR values in which two manufacturing routes exhibit identical performance; beyond these points one manufacturing route becomes more (or less) sustainable than another.

Looking at the CED analysis, using the curve associated with the conventional machining process as reference, the BEPs are found at SCR values of 0.28, 0.38, and 0.45 for the WAAM-based, internal symbiotic, and external symbiotic approaches, respectively. All additive manufacturing-based strategies have an energy advantage over traditional machining for SCR values below 0.28, as suggested by this. While the conventional WAAM-based process ceases to be advantageous beyond a SCR of 0.28, the symbiotic approaches remain favorable up to SCR values of 0.38 and 0.45 for the internal and external symbiotic cases, respectively. Another BEP is present between the two symbiotic strategies, specifically, the internal approach becomes more energy-efficient at SCR = 0.54.

In general, as SCR increases, both the WAAM-based and the external symbiotic strategies exhibit increasing energy consumption trends. The distance between these two curves becomes greater as for high SCR values the amount of material to be deposited through WAAM is substantial and it has a significant impact on the energy for material production, which, in turn, is absent in the symbiotic approaches. This behavior can be explained by the fact that higher SCR values correspond to thicker wall geometries, requiring more deposition volumes in additive processes. The machining approach shows, instead, an almost constant energy consumption trend. It starts with a fixed workpiece geometry, with variations in SCR affecting only the amount of material to be removed. Although this leads to increased material waste, the corresponding rise in processing energy remains relatively limited, as CED in subtractive processes is more strongly influenced by the amount of involved material rather than by the processing energy. For WAAM-based process, although its SEC is not particularly high, the long processing times, due to relatively low deposition rates compared to the Material Removal Rate (especially during roughing operations), can lead to higher total energy demand. Additionally, the impact of gas consumption during deposition is significant, and increases as the wall's thickness increases. For the external symbiotic path, the energy requirement is lower than WAAM-based, since hot extrusion and wire drawing are not included in the pre-manufacturing step. The impact of solid-state recycling is inside the pre-manufacturing stage (Cleaning + FSE).

Switching to the internal symbiosis strategy proposed in this work, the energy consumption trend is not linear: it initially increases with SCR and subsequently decreases. This behavior is primarily driven by the balance between the amount of material that needs to be removed and deposited. At lower SCR values, high material removal combined with substantial deposition leads to higher energy demand. As the SCR increases, based on the starting workpiece height, the required deposition volume decreases, and the need for material removal decreases, as machining produces a larger portion of the lower section of the vertical wall. This results in lower energy demand compared to additive-based strategies, which require more energy input for material deposition.

Looking instead at the cost results, the machining approach is almost always the cost-effective option, as only a single BEP can be identified between machining and WAAM-based. This BEP occurs at a very low SCR value (0.17), meaning that the WAAM-based approach is more convenient than milling only if a thin wall must be produced. It is also noticeable that machining costs remain almost constant as SCR varies, with a slight decrease as SCR increases. This behavior can be explained by examining the evolution of the different cost components with SCR. Material cost remains unchanged, as the input workpiece is the same for all SCR values, while the components that vary are the roughing and finishing costs. These costs depend on processing times, which in turn are determined by the material removal rate (MRR) and by the mass to be removed. Roughing time is characterized by high MRR values combined with large material removal, whereas finishing time is associated with low MRR values and very small removal volumes. Consequently, as SCR increases, roughing times decrease while finishing times increase (due to the larger finishing surface on top of the substrate), leading to a compensation effect that results in an overall machining cost that remains approximately constant. Additionally, the shift observed between SCR = 0.9 and SCR = 1 in the machining approach is due to the fact that SCR = 1 represents a boundary condition. In this situation, the total cost is dominated by the material cost alone, as no rough machining is required and the final geometry of the part essentially matches that of the input workpiece.

Another BEP that can be identified is between the WAAM-based and the internal approach. It indicates that after SCR = 0.48, the internal approach is more economically

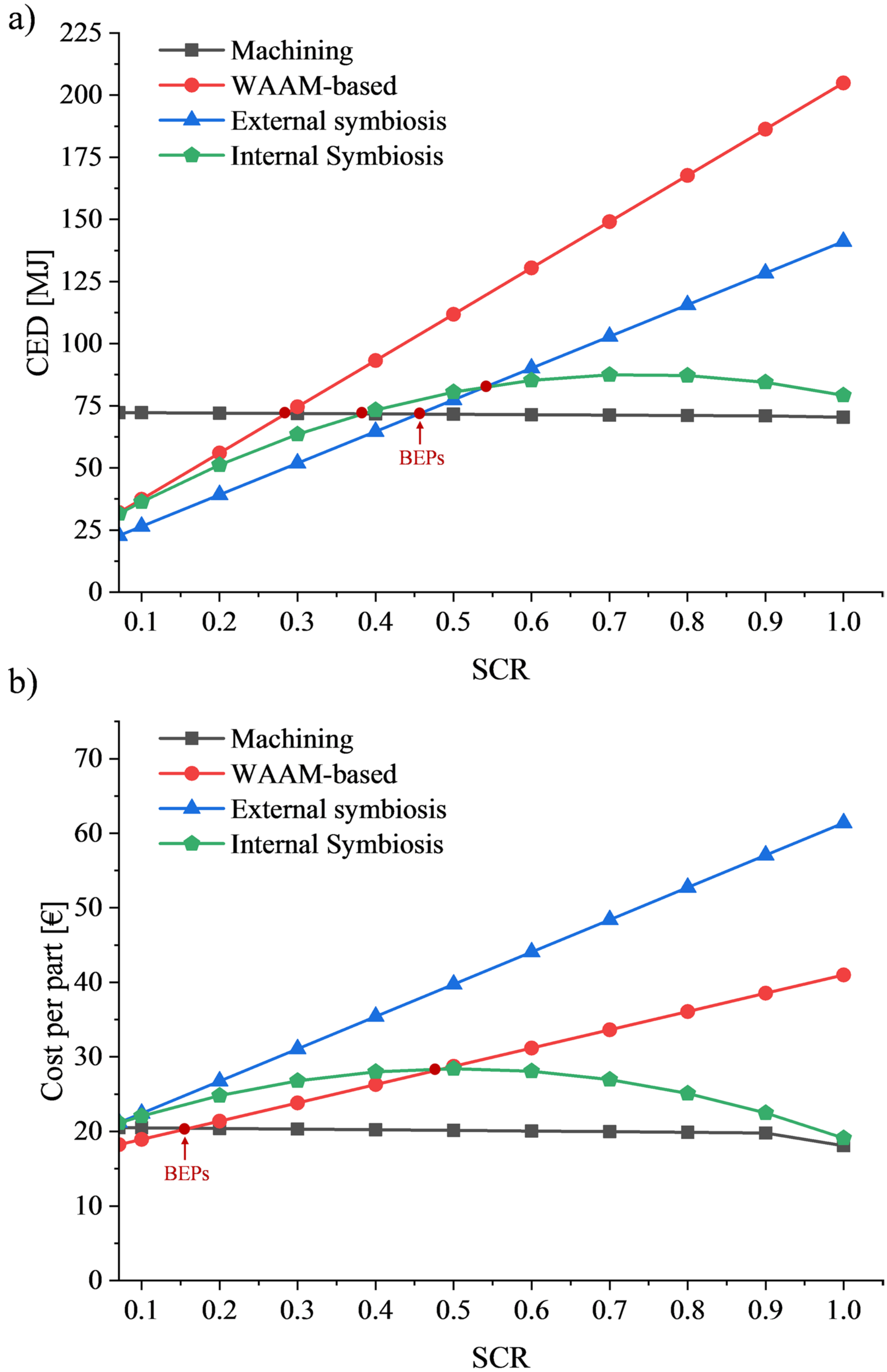

Fig. 7 Results of (**a**) CED, and (**b**) Cost per part as a function of the SCR

convenient than both the WAAM-based and the external symbiotic approach. When comparing the WAAM-based with the external symbiotic approach the trend observed is the opposite of that seen for CED. This inversion is primarily due to the cost modeling assumptions, which, as previously mentioned, account for the presence of multiple production steps when they are performed in-house. Conversely, in the WAAM-based route the wire feedstock is purchased in a form that is already suitable for direct deposition, thus only material procurement cost is considered neglecting further indirect and processing costs. Following the same rationale, the internal approach considers three production steps, but the amount of chips to be machined and preprocessed is quite low, therefore indirect costs do not significantly affect the results.

4.2 Sensitivity analysis and scenario analysis

The input data used to carry out the analysis are mainly case-specific, especially for cost estimation. Therefore, to assess the robustness of results, a sensitivity analysis was conducted by considering the effects of price fluctuations in cost analysis. Specifically, energy and material prices have been varied according to current market data. For electricity price, analysis was conducted with the highest and the lowest price for non-household consumers registered in EU in the second half of 2024. Therefore, 0.2578 €/kWh and 0.0767 €/kWh (for Cyprus and Finland) [47] have been used. Material cost is subject to market price fluctuation, which typically depends on the scarcity of the material. Data related to the market closing price of aluminum alloy in the first half of 2025 have been collected [51], revealing a standard deviation of approximately 18%. The results show that variations in energy prices have a negligible effect on the overall production cost, due to the relatively low contribution of electricity consumption to the total cost per part. Considering material price fluctuation, only minor shifts are observed in the cost curves. Nevertheless, these variations do not significantly shift the comparative ranking between the approaches, and the overall trends remain consistent with the baseline scenario. Specifically, the symbiotic approaches showed negligible sensitivity to price fluctuations. In the external case, this is due to the low market value

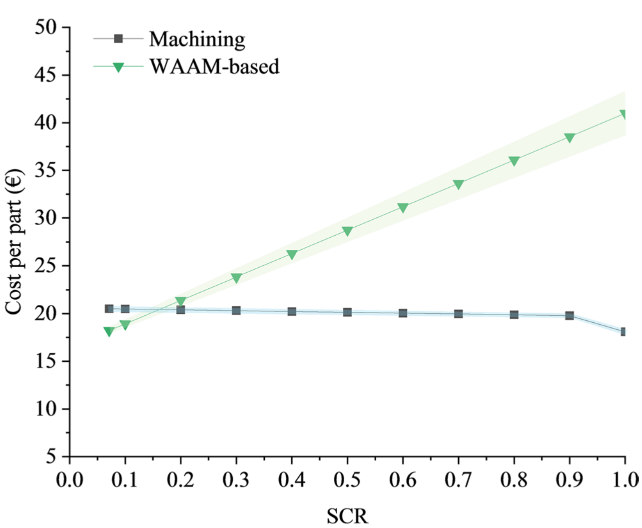

Fig. 8 Sensitivity of production cost to price fluctuations, represented as error bands

of chips, while in the internal scenario, only the oversized substrate eight is subject to purchase. Therefore, for ease of visualization, Fig. 8 includes only the error bands related to machining and WAAM-based approaches.

It is worth noting, however, that under very different market conditions, such as a surge in material prices, the cost advantage of the machining approach could be significantly diminished, potentially altering the economic competitiveness across the manufacturing scenarios.

To further investigate the economic potential of the external symbiotic pathway at an industrial scale, a prospective scenario analysis was conducted by varying the extrusion rate of the FSE process. As previously mentioned, at the current laboratory-scale configuration, the extrusion rate remains a non-optimized parameter and represents one of the factors influencing the total cost per part. The main limitation arises from the restricted vertical force available in the machine tool considered here, which is not specifically designed for FSE operations. Previous studies have demonstrated that higher extrusion rates can be achieved using more powerful equipment [19]. Specifically, the extrusion rate was increased by factors of 2×, 3× and 4× to the baseline value (1×), in order to assess the conditions under which the external symbiotic pathway could achieve cost parity with, or outperforms, the WAAM-based approach.

The results of this analysis are illustrated in Fig. 9, which reports the cost per part as a function of the SCR only for the WAAM-based and the external symbiotic scenarios. The machining-based approach and the internal symbiotic pathway are excluded from this comparison, as the former continued to yield the lowest cost across all configurations, making it unrealistic to identify an extrusion rate at which the symbiotic pathway would outperform it, while the latter exhibited only marginal improvements relative to its baseline value. The extrusion rate, is defined as E = n×, where n represents the scaling factor applied to the reference laboratory-scale extrusion rate reported in Table 1.

With the baseline extrusion rate (E = 1×), the external symbiotic pathway entails a substantially higher cost per part across the entire SCR range. However, as the extrusion rate increases, the external symbiotic cost curves converge progressively toward the WAAM-based reference. In particular, with a 3× increase in the extrusion rate, the external symbiotic pathway achieves near-parity with the WAAM-based scenario. By further increasing the extrusion rate to E = 4×, the external symbiosis outperforms the WAAM-based over the majority of the SCR range, suggesting that improvements in extrusion rate could make the external symbiotic pathway economically viable at an industrial scale. It is worth mentioning that such hypothetical improvements would reduce also the SEC making the symbiotic processes even more energy efficient.

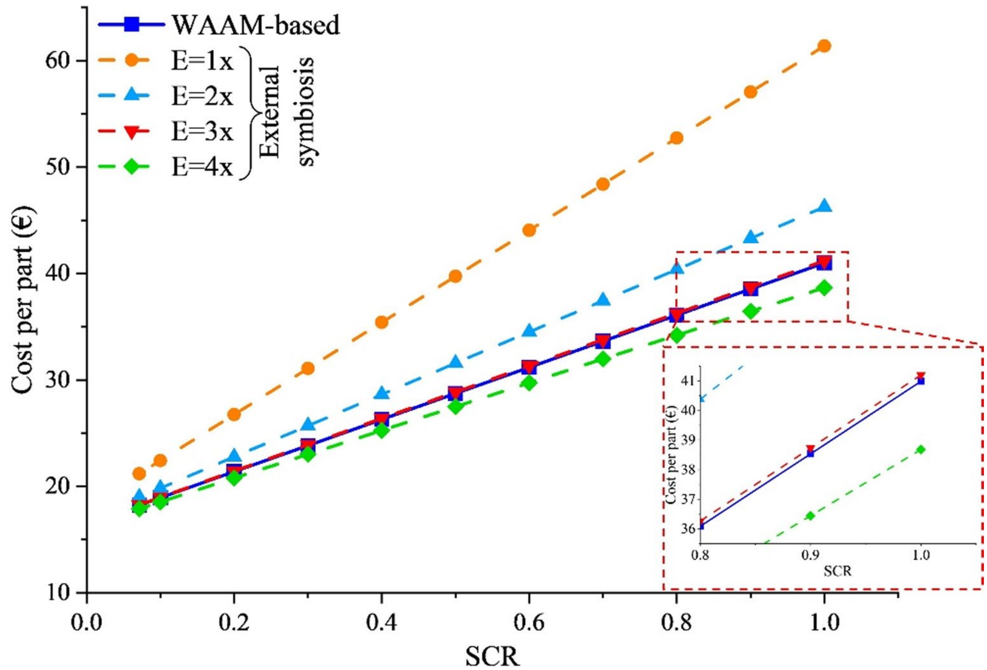

Fig. 9 Cost per part (€) as a function of the SCR for the WAAM-based approach and the external symbiosis route at varying extrusion rate multipliers (E = 1×, 2×, 3×, 4×)

5 LCA analysis

The results of the LCA are presented in this section. The ReCiPe 2016 Endpoint (H) methodology was adopted in order to evaluate the environmental impacts across different impact categories. The assessment framework considers 18 midpoint indicators (global warming, fine particulate formation, water consumption, etc…) to capture and quantify the contributions of individual environmental processes [52].

The four manufacturing routes previously introduced were implemented in the SimaPro software [39] to perform the LCA analysis. The adoption of the ReCiPe methodology enables the identification of trends that differ from those obtained using the CED indicator, as it accounts for the combined contribution of multiple midpoint impact categories. This integrated perspective allows the environmental performance of different manufacturing routes to be assessed across multiple impact categories. As a result, it highlights the influence of the chosen impact assessment method beyond a single energy-based metric.

The analysis is performed considering the two levels of complexity already examined in this study, in order to assess whether the LCA results are consistent with those obtained from the CED analysis. From the authors' perspective, these two case studies represent two extreme scenarios that can highlight different behaviors of the four manufacturing routes under investigation. As shown in Fig. 10, a slightly different trend compared to the CED results can be observed. For a SCR equal to 0.2, the ranking of the manufacturing routes remains unchanged: the external symbiotic approach exhibits the lowest environmental impact, while machining represents the worst-performing option. Instead, for SCR = 0.8, the external symbiotic route continues to be the most environmentally favorable solution. This outcome differs from the CED perspective, in which machining appears to be the best-performing route. These differences can be attributed to the distinct weighting of contributing factors across impact assessment methodologies. In the ReCiPe approach, material-related impacts play a dominant role, whereas electricity consumption contributes relatively less to the overall results. This behavior is mainly driven by the human carcinogenic impact category, which is strongly associated with material production. In the case of aluminum indeed, the processes associated with its production (thus the bauxite mining, refining and electrolysis) are not only energy-intensive but also associated with potential emissions of carcinogenic substances. Furthermore, pollutant emissions generated during heat production and electricity generation contribute significantly to the overall increase in toxic emissions. As a consequence, increasing the SCR from 0.2 to 0.8 leads to an increase in the CED of the external symbiotic process, mainly due to the higher electricity demand associated with FSE and WAAM process. However, under the ReCiPe framework, the external symbiotic route continues to outperform machining, whose impact remains approximately constant, due to the comparatively lower material-related environmental burden. A similar divergence between CED- and ReCiPe-based results have been reported in previous studies [53].

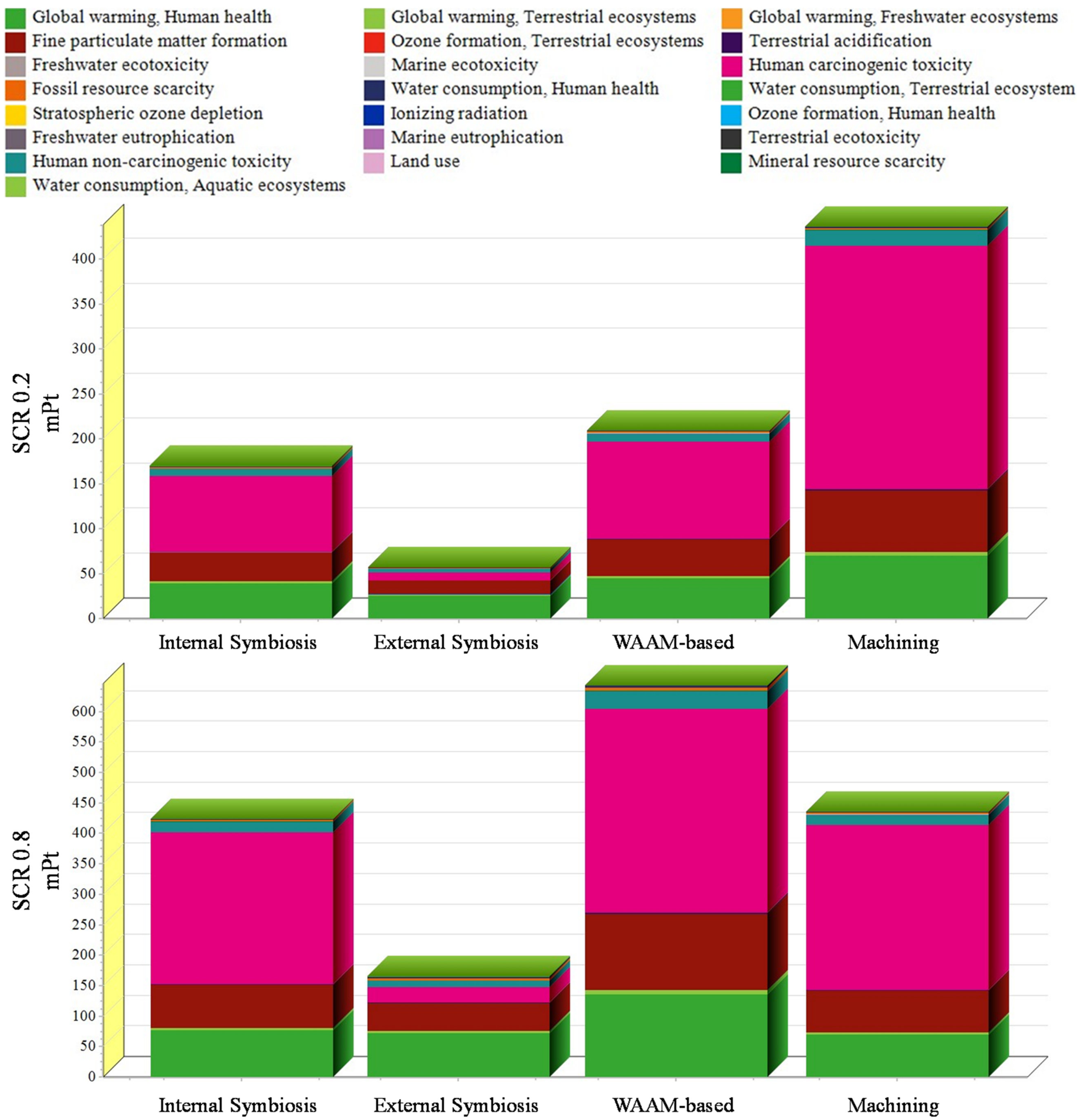

Fig. 10 ReCiPe2016 Endpoint (H) per impact category characterization – comparative results of the four manufacturing strategies for SCR 0.2 and 0.8

6 Conclusions and future outlooks

The presented study proposed a comparative assessment of four manufacturing strategies for a T-shaped aluminum component, focusing on both environmental and economic performance by using CED and production cost as metrics, respectively. With respect to prior studies that have predominantly focused on single manufacturing routes (e.g., FSE [19, 27]) or on isolated assessments of economic or environmental performance, this study developed a comprehensive modelling framework that captures the entire process chain, from material recovery to final component production, introducing a novel comparison between internal and external symbiotic manufacturing strategies, adding a new dimension to the evaluation of energy performance in hybrid manufacturing methods, with a focus on industrial symbiosis implementation.

The analyzed manufacturing routes include: (i) a full machining approach, (ii) a WAAM-based approach using conventionally manufactured wire, and two industrial symbiosis strategies always based on WAAM deposition, namely: (iii) external symbiosis, using chips generated from third-parties machining operations, (iv) internal symbiosis, based on in-house generated chips. The process enabling the symbiotic link between machining and WAAM is the Friction Stir Extrusion (FSE).

The main conclusions coming from the analyses carried out in this work are summarized below:

- When a high shape complexity is considered, thus when SCR = 0.2, from the energetic point of view the external symbiotic approach demonstrated the lowest CED, due to low contribution of the raw material embodied energy. Conversely, for a low geometrical complexity, such as when SCR = 0.8, machining approach is the most energy efficient choice;
- The internal symbiotic approach can represent a favorable strategy when the input workpieces are available with a height greater than that of the substrate region but lower than the final height of the vertical wall. In such cases, it is possible to avoid purchasing either a taller initial semi-finished product, as required by the conventional machining process, or one matching the height of the substrate alone;
- Both symbiotic approaches presented in this study appear to be valid candidates for minimizing metal waste generated during the production of mechanical components. Specifically, the external symbiotic approach reuses scrap originating from third-party companies, while the internal symbiotic approach minimizes waste generated within the company itself;
- From a cost perspective, machining remains the most cost-effective approach across most of the SCR scenarios, as it requires only one production step. WAAM-based and symbiotic routes instead involve higher operational complexity in production leading to increased indirect and labour costs;
- The low productivity of the current FSE setup significantly impacts the feasibility of symbiotic routes, as its low extrusion rate drives up processing times. In particular, indirect and labour costs dominate the total cost structure, and they are highly sensitive to processing times. Despite its current limitations, FSE holds strong potential for enabling circular and energy-efficient manufacturing routes, especially if scaled and optimized for industrial application. In fact, some of the authors have shown that FSE systems capable of operating under higher vertical loads can markedly increase the extrusion rate, which in turn leads to a substantial reduction in the specific energy consumption required for the process [19].
- Internal symbiosis shows cost improvements at higher SCR, due to reduced deposition and milling volumes, which lower processing time and indirect costs;
- The extension of the analysis with varying SCR revealed the presence of break-even points where the competitiveness of each route shifts, emphasizing the importance of geometry complexity in decision-making;
- A sensitivity analysis confirmed that actual energy price fluctuations have a minimal influence on results, while material price variations introduce small shifts in cost curves without altering the overall trends;
- An LCA analysis conducted using the ReCiPe methodology confirms that sustainability assessment is highly dependent on the chosen perspective, as different impact assessment methods may lead to different outcomes. When material-related impacts represent the dominant contribution, the external symbiotic route emerges as the most environmentally favorable solution, regardless of the SCR value.

It is important to note that the results are derived from a specific case study; however, the adoption of the SCR as a complexity indicator enables partial generalization of the findings to different geometries. The proposed model can be extended to other materials and industrial contexts, provided that reliable data on embodied energy and process-specific energy consumption are available. Nonetheless, variations in alloy type, machine performance, and geographic context may influence the identified BEPs. From a practical perspective, the model and the identified BEPs can support manufacturing engineers in selecting the most suitable production route by linking part complexity (via SCR) to energy and cost performance. This study still presents some limitations that should be acknowledged. The economic analysis is limited to production costs, without accounting for logistics (and reverse logistics) costs. In this respect, the internal symbiotic approach proposed in this work could offer significant advantages by reducing transportation needs and handling complexity, thereby potentially lowering overall costs. It should also be noted that tool wear has not been explicitly included in the economic assessment as it was considered negligible. At industrial scale, this factor may represent a non-negligible cost contribution for FSE-based processes, potentially shifting the cost BEPs.

Finally, the analysis does not consider external incentives or policy support that could accompany the adoption of industrial symbiosis practices. Including these factors in future studies could substantially shift the cost-benefit balance in favor of symbiotic approaches with a more comprehensive and policy-aligned perspective.

Acknowledgements This study was carried out within the MICS (Made in Italy – Circular and Sustainable) Extended Partnership and received funding from the European Union Next-Generation EU (PIANO NAZIONALE DI RIPRESA E RESILIENZA (PNRR) – MISSIONE 4 COMPONENTE 2, INVESTIMENTO 1.3 – D.D. 1551.11–10-2022, I.D.: PE00000004, CUP: B73C22001270006).

Funding Open access funding provided by Università degli Studi di Palermo within the CRUI-CARE Agreement.

Declarations

Conflict of interest The Authors disclose no actual or potential conflict of interest that could inappropriately influence, or be perceived to influence, this work.

References

1. Environmental profile report for the european aluminium industry (2024) - Full Report Life Cycle Inventory (LCI) data for aluminium production and transformation processes in Europe
2. IEA, International Energy Agency: World Energy Outlook (2024)
3. International Aluminium Institute global aluminium cycle 2024 n.d. https://alucycle.international-aluminium.org/public-access/public-global-cycle/
4. Atherton J (2007) Declaration by the Metals Industry on Recycling Principles. Int J Life Cycle Assess 12:59–60. https://doi.org/10.1065/lca2006.11.283
5. Cooper DR, Song J, Gerard R (2018) Metal recovery during melting of extruded machining chips. J Clean Prod 200:282–292. https://doi.org/10.1016/j.jclepro.2018.07.246
6. Xiao Y, Reuter MA (2002) Recycling of distributed aluminium turning scrap. Min Eng 15:963–970. https://doi.org/10.1016/S0892-6875(02)00137-1
7. Van Geertruyden WH, Prescott CA, Misiolek WZ, Peterson R (2005) Evaluation of light gauge Al scrap remelting after consolidation via the extrusion process. Light Metal Age 63:14–18
8. Rahimi H, Sabour MR, Taherkhani E, Faraji G (2025) A comprehensive review on solid-state recycling of titanium for sustainable engineering applications. Results Eng 27:107056. https://doi.org/10.1016/j.rineng.2025.107056
9. Sabour MR, Taherkhani E, Rezaei AR, Zohrevand M, Safahi H, Faraji G (2024) Solid-state recycling of magnesium and its alloys via plastic deformation: An overview of processing and properties. J Mater Res Technol 31:3117–3148. https://doi.org/10.1016/j.jmrt.2024.07.032
10. Duflou JR, Tekkaya AE, Haase M, Welo T, Vanmeensel K, Kellens K et al (2015) Environmental assessment of solid state recycling routes for aluminium alloys: can solid state processes significantly reduce the environmental impact of aluminium recycling? CIRP Ann Manuf Technol 64:37–40. https://doi.org/10.1016/j.cirp.2015.04.051
11. Ingarao G, Priarone PC, Deng Y, Paraskevas D (2018) Environmental modelling of aluminium based components manufacturing routes: Additive manufacturing versus machining versus forming. J Clean Prod 176:261–275. https://doi.org/10.1016/j.jclepro.2017.12.115
12. Frosch RA, Gallopoulos NE (1989) Strategies for Manufacturing. Sci Am 261:144–152. https://doi.org/10.1038/scientificamerican0989-144
13. Duflou JR, Wegener K, Tekkaya AE, Hauschild M, Bleicher F, Yan J et al (2024) Efficiently preserving material resources in manufacturing: industrial symbiosis revisited. CIRP Ann 73:695–721. https://doi.org/10.1016/j.cirp.2024.05.006
14. Kalashnikov K, Campanella D, Ingarao G, Buffa G, Fratini L, Micari F (2025) Exploring the feasibility of a closed-loop industrial symbiosis link through Friction Stir Extrusion-based Additive Manufacturing. CIRP Ann 74:339–343. https://doi.org/10.1016/j.cirp.2025.03.042
15. Carvalho GHSFL, Campatelli G, Fratini L (2024) Feasibility study of using friction stir extruded recycled aluminum rods for welding and additive manufacturing. Manuf Lett 42:52–55. https://doi.org/10.1016/j.mfglet.2024.10.007
16. Baruah S, Hoekstra J, Schmitz T (2025) An activity-based parametric cost analysis for upcycling machining chips to produce feedstock for sustainable additive friction stir deposition. Addit Manuf Lett 14:100288. https://doi.org/10.1016/j.addlet.2025.100288
17. Stotz PM, Niero M, Bey N, Paraskevas D (2017) Environmental screening of novel technologies to increase material circularity: A case study on aluminium cans. Resour Conserv Recycl 127:96–106. https://doi.org/10.1016/j.resconrec.2017.07.013
18. Paraskevas D, Kellens K, Dewulf W, Duflou JR (2015) Environmental modelling of aluminium recycling: a Life Cycle Assessment tool for sustainable metal management. J Clean Prod 105:357–370. https://doi.org/10.1016/j.jclepro.2014.09.102
19. Baffari D, Reynolds AP, Masnata A, Fratini L, Ingarao G (2019) Friction stir extrusion to recycle aluminum alloys scraps: Energy efficiency characterization. J Manuf Process 43:63–69. https://doi.org/10.1016/j.jmapro.2019.03.049
20. Ingarao G, Amato M, Latif A, La Rosa AD, Di Lorenzo R, Fratini L (2023) Life cycle assessment of aluminum alloys chips recycling through single and multi-step friction stir consolidation processes. J Manuf Syst 68:651–9. https://doi.org/10.1016/j.jmsy.2023.05.021
21. Ingarao G, Priarone PC (2020) A comparative assessment of energy demand and life cycle costs for additive- and subtractive-based manufacturing approaches. J Manuf Process 56:1219–1229. https://doi.org/10.1016/j.jmapro.2020.06.009
22. Morrow WR, Qi H, Kim I, Mazumder J, Skerlos SJ (2007) Environmental aspects of laser-based and conventional tool and die manufacturing. J Clean Prod 15:932–943. https://doi.org/10.1016/j.jclepro.2005.11.030
23. Hammond G, Jones C, Lowrie F, Tse P (2011) Embodied carbon : the Inventory of Carbon and Energy (ICE). BSRIA
24. Borda F, La Rosa AD, Filice L, Gagliardi F (2023) Environmental impact of process constrained topology optimization design on automotive component' life. Int J Mater Form 16:48. https://doi.org/10.1007/s12289-023-01771-2
25. Bölükbaşı ÖS, Serindağ T, Gürol U, Günen A, Çam G (2023) Improving oxidation resistance of wire arc additive manufactured Inconel 625 Ni-based superalloy by pack aluminizing. CIRP J Manuf Sci Technol 46:89–97. https://doi.org/10.1016/j.cirpj.2023.07.011
26. Gürol U, Altınay Y, Günen A, Bölükbaşı ÖS, Koçak M, Çam G (2023) Effect of powder-pack aluminizing on microstructure and

oxidation resistance of wire arc additively manufactured stainless steels. Surf Coat Technol 468:129742. https://doi.org/10.1016/j.surfcoat.2023.129742
27. Ingarao G, Baffari D, Bracquene E, Fratini L, Duflou J (2019) Energy demand reduction of aluminum alloys recycling through friction stir extrusion processes implementation. Procedia Manuf 33:632–8. https://doi.org/10.1016/j.promfg.2019.04.079
28. Priarone PC, Ingarao G (2017) Towards criteria for sustainable process selection: On the modelling of pure subtractive versus additive/subtractive integrated manufacturing approaches. J Clean Prod 144:57–68. https://doi.org/10.1016/j.jclepro.2016.12.165
29. Eurostat - Energy for final consumption n.d. https://ec.europa.eu/eurostat/statistics-explained/index.php?title=Calculation_methodologies_for_the_share_of_renewables_in_energy_consumption#Energy_available_for_final_consumption
30. Cao F, Gu Y, Wang D, Wang L, Liu Y, Chen S et al (2024) Effect of single and double stage homogenization treatments on microstructure and properties of wire+arc additively manufactured 2319 Al alloy. Mater Charact 217:114389. https://doi.org/10.1016/j.matchar.2024.114389
31. Priarone PC, Campatelli G, Montevecchi F, Venturini G, Settineri L (2019) A modelling framework for comparing the environmental and economic performance of WAAM-based integrated manufacturing and machining. CIRP Ann 68:37–40. https://doi.org/10.1016/j.cirp.2019.04.005
32. European Commission (2010) International Reference Life Cycle Data System (ILCD) Handbook-General guide for Life Cycle Assessment-Provisions and Action Steps. Publications Office of the European Union: Luxembourg 2010:150. Publications Office
33. Kara S, Li W (2011) Unit process energy consumption models for material removal processes. CIRP Ann 60:37–40. https://doi.org/10.1016/j.cirp.2011.03.018
34. Amantia S, Campanella D, Puleo R, Buffa G, Fratini L (2024) Effect of process parameters on the mechanical properties of wires produced from A356 aluminum alloy chips by Continuous Friction Stir Extrusion: Experiments and numerical simulation. CIRP J Manuf Sci Technol 54:28–42. https://doi.org/10.1016/j.cirpj.2024.08.001
35. Klein T, Schnall M (2020) Control of macro-/microstructure and mechanical properties of a wire-arc additive manufactured aluminum alloy. Int J Adv Manuf Technol 108:235–244. https://doi.org/10.1007/s00170-020-05396-6
36. Granta Design Limited (2025) CES Selector R1 2025 software
37. Amantia S, Kalashnikov K, Campatelli G, Fratini L, Ingarao G (2025) Life cycle assessment and energy characterization of friction surfacing deposition of aluminum alloys. J Manuf Syst 80:356–365. https://doi.org/10.1016/j.jmsy.2025.03.008
38. Buffa G, Campanella D, Adnan M, La Commare U, Ingarao G, Fratini L (2024) Improving the industrial efficiency of recycling aluminum alloy chips using Friction Stir Extrusion: thin wires production process. Int J Precis Eng Manuf Green Technol 11:1133–46. https://doi.org/10.1007/s40684-023-00573-w
39. SimaPro Craft 10.3
40. Priarone PC, Pagone E, Martina F, Catalano AR, Settineri L (2020) Multi-criteria environmental and economic impact assessment of wire arc additive manufacturing. CIRP Ann 69:37–40. https://doi.org/10.1016/j.cirp.2020.04.010
41. Kellens K, Mertens R, Paraskevas D, Dewulf W, Duflou JR (2017) Environmental Impact of Additive Manufacturing Processes: Does AM Contribute to a More Sustainable Way of Part Manufacturing? Procedia CIRP, vol. 61, Elsevier BV pp. 582–7. https://doi.org/10.1016/j.procir.2016.11.153
42. Laureijs RE, Roca JB, Narra SP, Montgomery C, Beuth JL, Fuchs ERH (2017) Metal additive manufacturing: cost competitive beyond low volumes. J Manuf Sci Eng. https://doi.org/10.1115/1.4035420
43. Campatelli G, Montevecchi F, Venturini G, Ingarao G, Priarone PC (2020) Integrated WAAM-Subtractive Versus Pure Subtractive Manufacturing Approaches: An Energy Efficiency Comparison. Int J Precis Eng Manuf - Green Technol 7:1–11. https://doi.org/10.1007/s40684-019-00071-y
44. Catalano AR, Priarone PC, Settineri L (2024) An economic evaluation of hybrid WAAM-subtractive manufacturing in relation to deposition process parameters. Procedia CIRP 122:49–54. https://doi.org/10.1016/j.procir.2024.02.003
45. Scrapmonster (n.d.). https://www.scrapmonster.com/
46. Baumers M, Dickens P, Tuck C, Hague R (2016) The cost of additive manufacturing: machine productivity, economies of scale and technology-push. Technol Forecast Soc Change 102:193–201. https://doi.org/10.1016/j.techfore.2015.02.015
47. Eurostat - Electricity price statistics (n.d.) https://ec.europa.eu/eurostat/statistics-explained/index.php?title=Electricity_price_statistics#Electricity_prices_for_non-household_consumers
48. Campatelli G, Campanella D, Barcellona A, Fratini L, Grossi N, Ingarao G (2020) Microstructural, mechanical and energy demand characterization of alternative WAAM techniques for Al-alloy parts production. CIRP J Manuf Sci Technol 31:492–499. https://doi.org/10.1016/j.cirpj.2020.08.001
49. Lekkala N, Siva Prasad K (2025) Investigation of mechanical and microstructural characteristics of Aluminum 6061 through wire arc additive manufacturing under as-deposited and post-heat-treated conditions. J Mater Eng Perform. https://doi.org/10.1007/s11665-025-11082-z
50. Kamps T, Lutter-Guenther M, Seidel C, Gutowski T, Reinhart G (2018) Cost- and energy-efficient manufacture of gears by laser beam melting. CIRP J Manuf Sci Technol 21:47–60. https://doi.org/10.1016/j.cirpj.2018.01.002
51. London Metal Exchange (2025) LME Aluminium Alloy – Price graphs. n.d. https://www.lme.com/Metals/Non-ferrous/LME-Aluminium-Alloy#Price+graphs
52. Huijbregts MAJ, Steinmann ZJN, Elshout PMF, Stam G, Verones F, Vieira M et al (2017) ReCiPe2016: a harmonised life cycle impact assessment method at midpoint and endpoint level. Int J Life Cycle Assess 22:138–47. https://doi.org/10.1007/s11367-016-1246-y
53. Amantia S, Kalashnikov K, Ingarao G, Lorenzo R, Di, Buffa G, Fratini L (2025) Comparative Environmental Impact Analysis of Friction-based Additive Manufacturing Techniques. Procedia CIRP 135:456–461. https://doi.org/10.1016/j.procir.2024.12.043